Chemical Science

Accepted Manuscript

This article can be cited before page numbers have been issued, to do this please use: H. Liu, Y. Fu, J. W. Y. Lam, B. Zhong Tang and Z. Zhao, *Chem. Sci.*, 2026, DOI: 10.1039/D6SC03065C.

ROYAL SOCIETY OF CHEMISTRY

rsc.li/chemical-science

View Article Online
DOI: 10.1039/D6SC03065C

Perspective

Purely organic room-temperature phosphorescence sensitizers for OLEDs

Hao Liu[a,c], Yan Fu[a], Jacky W. Y. Lam[c], Ben Zhong Tang[b,c] and Zujin Zhao[a]*

Received 00th January 20xx,
Accepted 00th January 20xx

DOI: 10.1039/x0xx00000x

Organometallic phosphorescent materials have been developed as the critical luminescent materials for organic light-emitting diodes (OLEDs). However, most purely organic room-temperature phosphorescence (RTP) materials without any hevay metals are still lack of competitiveness in OLEDs. Recently, significant progresses have been made in purely organic RTP materials, and their electroluminescence (EL) performances become comparable to those of traditional phosphorescent complexes. In this perspective, the advancements and proposed design strategies of the efficient purely organic RTP materials are summarized. Furthermore, the promising application of these RTP materials as sensitizers for narrow-spectrum multi-resonance emitters is also discussed and outlooked, which is conducive to the development of high-resolution OLEDs. It is expected that this perspective will provide valuable guidelines for advancing robust purely organic RTP sensitizers and further promote the OLED industry.

Introduction

Organic luminescent materials have been developed for over half a century, and have play a crucial role in organic light-emitting diodes (OLEDs),[1,2] secure communications,[3] encryption,[4,5] bioimaging,[6,7] etc. Due to the spin statistics of electrons, electro-generated excitons consist of 75% of triplet states and 25% of singlet states, where the triplet states are kinetically hindered from converting to singlet states or ground states.[8] One of the most successful strategies for utilizing triplet excitons is the phosphorescent organometallic complexes, which generally incorporate heavy metals (e.g., Ir, Pt) to enhance spin-orbit coupling (SOC).[9,10] They can achieve nearly 100% exciton utilization efficiency (EUE), and the extraordinary performance attract considerable interest across multiple fields.[11,12] The most successful application of these phosphorescent materials is in OLEDs, which have taken large market shares of mobile displays.[13] Nevertheless, the presence of expensive heavy metals brings about challenges to cost control of OLEDs, necessitating the development of low-cost purely organic luminescent materials.

Recently, several types of high-EUE purely organic luminescent materials featuring distinct mechanisms have been proposed, including room-temperature phosphorescence (RTP),[14] thermally activated delayed fluorescence (TADF),[15] hybrid locally and charge transfer (HLCT),[16] and organic radicals.[17] TADF materials typically consist of electron donor (D) and acceptor (A) moieties, wherein the D–A structure can induce intramolecular charge transfer (ICT) characteristics.[18] The reverse intersystem crossing (RISC) facilitates the conversion of excitons from the lowest triplet (T_1) state to lowest singlet (S_1) state, enabling nearly 100% EUE and impressive electroluminescence (EL) performance of exceeding 30%.[19-22] This TADF characteristic was also discovered in polycyclic aromatic compounds constructed by alternating heteroatoms with opposite electronegativities, termed as multi-resonance (MR) TADF materials.[23-25] Such MR-TADF materials can realize narrow-spectrum emission, which is regarded as the ideal terminal emitters for high-definition displays.[26-28] However, the rates of RISC (k_{RISC}s) of MR-TADF molecules remain relatively low due to the insufficient separation of the frontier molecular orbitals, which results in a large energy gap (ΔE_{ST}) between S_1 and T_1 states.[29] Thus, sensitization strategy was proposed to enhance the EL efficiency and operational stability of MR-TADF emitters, where the TADF or metallic phosphorescent materials are employed as sensitizers.[30-34] However, the possible repeated cycles between S_1 and T_1 states of TADF materials may lead to prolonged exciton lifetimes and inevitable non-radiative loss.[35] On the other hand, purely organic RTP emitters are potentially applicable in sensitized OLEDs due to the high EUE. Notably, the unidirectional radiative decay characteristics of RTP materials minimize the spin-flip cycles between triplet and singlet states, which is favourable for increasing the efficiency and stability of the devices. Recently, some RTP materials have been applied to those sensitized OLEDs that utilize narrow-spectrum fluorescent materials as terminal emitters.[36,37] Meanwhile, the purely organic RTP materials contain no expensive metals, which can effectively reduce the cost of materials and thus facilitate application in OLED panels.

[a] State Key Laboratory of Luminescent Materials and Devices, Guangdong Provincial Key Laboratory of Luminescence from Molecular Aggregates, South China University of Technology, Guangzhou 510640, China. E-mail: mszjzhao@scut.edu.cn
[b] Guangdong Basic Research Center of Excellence for Aggregate Science, School of Science and Engineering, The Chinese University of Hong Kong (Shenzhen), Longgang, Shenzhen, Guangdong 518172, China.
[c] Department of Chemistry and the Hong Kong Branch of Chinese National Engineering Research Center for Tissue Restoration and Reconstruction, The Hong Kong University of Science and Technology, Clear Water Bay, Kowloon, Hong Kong 999077, China.

Although purely organic RTP materials offer several advantages over TADF materials, the realization of efficient phosphorescent emission from them still remains challenging. Over the past decade, various strategies for enhancing RTP in organic materials have been proposed.[38,39,40] However, numerous RTP materials can only function efficiently under specific conditions. For example, crystallization is a commonly used method to rigidify organic molecules and stabilize triplet states.[41] In OLED fabrication, the vacuum evaporation and solution-processed technology are widely used, whereby amorphous films are utilized as the emissive layers.[1,42] Moreover, to ensure the reproducibility and stability of OLEDs, the use of additives to facilitate RTP emission should be avoided.[43] As a result, several conventional purely organic RTP emitters only provided low EUEs in OLEDs,[44,45] which could be attributed to inefficient ISC and slow phosphorescent decay rate. Therefore, the application of purely organic RTP materials in OLEDs still face several obstacles.

To date, the researches on purely organic RTP materials mainly focus on molecular design strategies and their photophysical properties, and the scarcity of reports on their EL performance impedes the progress of RTP-based OLEDs. Herein, we review the recent advancements in purely organic RTP materials and their corresponding EL performances. The effective strategies to facilitate RTP emissions are summarized, and the progress of EL performances of these RTP emitters are also introduced. More importantly, the key factors governing high EL performances in RTP materials and their potential application as purely organic sensitizers are systematically analysed and discussed, with prospective developing paths being proposed.

Design principles of RTP materials

Photophysical process in RTP materials

The Jablonski diagram is widely used to understand the generation and deactivation pathways of singlet and triplet excitons (Fig. 1). Under photoexcitation, normally only singlet excitons are generated according to the principle of spin conservation. Thus, the triplet excitons can only be generated through ISC from singlet manifold. The excitons at higher-lying singlet or triplet states will rapidly relax to lowest S_1 and T_1 states via internal conversion (IC) processes. Besides, the ISC from S_1 to higher-level triplet states followed by IC can also effectively populate the T_1 states.

Notably, the T_1 state is inherently susceptible to deactivation through various competitive pathways. Beyond internal non-radiative decay, such as vibrational dissipation[46] and RISC, or triplet-triplet annihilation (TTA) and singlet-triplet annihilation (STA),[47] triplet excitons in purely organic systems are highly sensitive to quenching by molecular oxygen ($^3O_2$) under ambient conditions.[48] This process is governed by triplet-triplet energy transfer, wherein the interaction between the T_1 state of the luminophore and the triplet ground state of oxygen

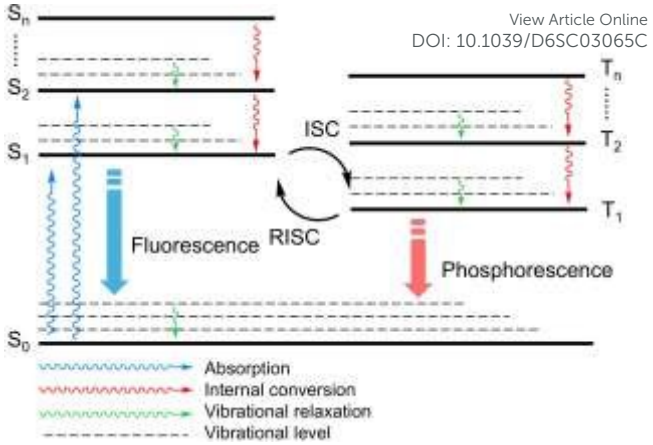

Fig. 1 Jablonski diagram for photophysical processes.

leads to the formation of singlet oxygen and the non-radiative deactivation of the molecule. Consequently, achieving efficient RTP requires synergistic effects: employing rigid matrices or crystalline packing to provide an effective oxygen barrier and minimize non-radiative loss while increasing SOC constant for achieving high radiative rate (k_P) and ISC rate (k_{ISC}), which are essential for maximizing photoluminescence quantum yields (Φ_{PL}s). So, the design principles for efficient RTP materials primarily involve two aspects: Firstly, optimizing the morphology and host matrix to suppress non-radiative decay and modulate intermolecular interactions. Secondly, enhancing SOC to facilitate spin-flip processes between singlet and triplet states, as well as between triplet and ground states.

Morphology dependence of RTP materials

Crystallization. Many of the RTP phenomena were observed in aqueous solutions during the early stages of the development. Although the phosphorescence in anthracene crystals had been reported in 1960s,[49] its weak intensity under ambient conditions limited its practical application. Rigid polymer matrix can effectively restrict molecular motions, facilitating phosphorescent emissions. Ghiggino et al. observed phosphorescent emissions of tryptophan by doping it into rigid polyvinyl-alcohol (PVA) matrix.[50] Levy et al. processed dyes doped sol-gel silica glasses, where the RTP phenomena were detected.[51] In 2010, Tang et al. reported a series of halogenated benzophenone derivatives which can only present strong phosphorescence in single crystals, namely crystal-induced phosphorescence (Fig. 2).[41] Even though the carbonyl group and halogens are favoured to increase SOC constants, the molecular rotations in solutions or amorphous films induced the severe exciton quenching. Crystallization effectively restricts intramolecular motions through an extensive network of hydrogen bonds. Consequently, 4,4'-difluorobenzophenone (DFBP) molecule achieved persistent phosphorescence with a long lifetime (τ_P) of 1.3 ms and a high phosphorescent quantum yield (Φ_P) of 40%. Huang et al. designed 2,4,6-trimethoxy-1,3,5-

View Article Online
DOI: 10.1039/D6SC03065C

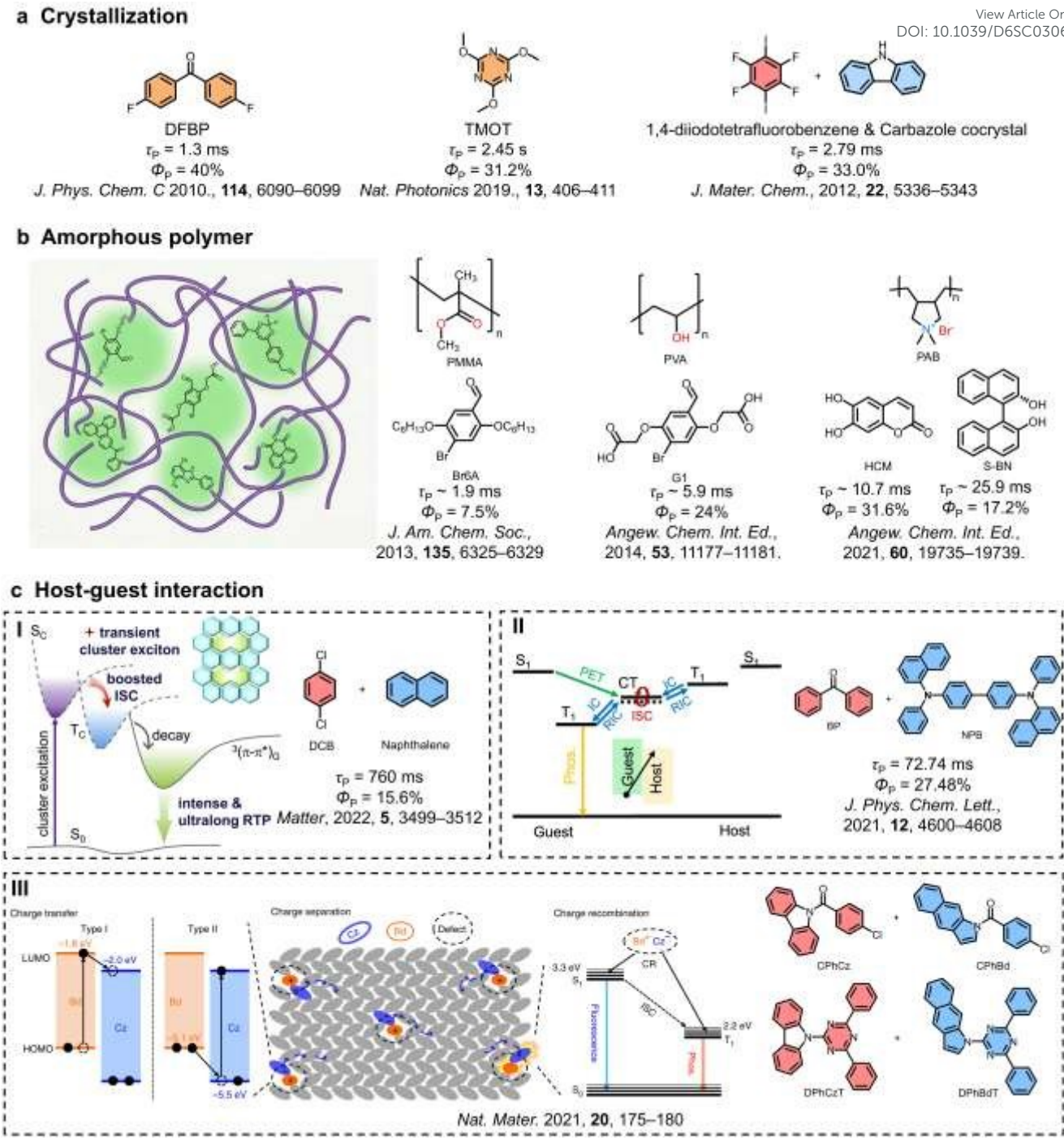

Fig. 2 Examples of morphology dependence of RTP materials: (a) crystallization induced phosphorescence, (b) RTP in amorphous polymer matrix and (c) host-guest interaction and their mechanisms, the red molecules represent host phase and blue molecules are dopants: I) Phosphorescent decay via intermolecular orbitals. Reproduced with permission: Copyright 2022, Elsevier.[60] II) Photoinduced electron transfer. Reproduced with permission: Copyright 2021, American Chemical Society.[62] III) Charge-separated states induced afterglow. Reproduced with permission: Copyright 2021, Springer-Nature.[61]

triazin (TMOT) derivatives and proposed H-aggregation assisted ultra-long phosphorescent emission.[52] The dimeric states of H-aggregates can effectively stabilize triplet states of TMOT, bringing about a long τ_P of 2.45 s and a good Φ_P of 31.2%. Besides, several RTP phenomena were observed in organic co-crystals. For example, Jin et al. adopted halogen-rich compound 1,4-diiodotetrafluorobenzene and carbazole to grow co-crystalline structures, which utilized C–I···π interactions to promote phosphorescent emission. The suspension microparticles of co-crystal exhibited a τ_P of 2.79 ms and a Φ_P of 33.0%, respectively.[53]

Amorphous polymer. Polymerization is an effective method to increase inter/intra-molecular interactions, where the

stabilization of environment is favoured for RTP emission. **Fig. 2c** displays some examples of RTP emissions in amorphous polymer matrix. Poly(methyl methacrylate (PMMA) is a widely used host matrix for the encapsulation of RTP materials,[54,55] where the glassy state provides a rigid microenvironment. For hydrophilic emitters, PVA is a more appropriate selection where the strong hydrogen bonding can be established.[56] Besides, other kinds of polymers, such as polyacrylamide[57] and polyamide 6,[58] are also the candidates for RTP matrix. Ionic bonding polymers are emerging as the ideal matrix for long-lived RTP emissions, since the strong electrostatic interactions between opposite ions can greatly stabilize triplet excitons. Ma et al. developed a series of new RTP systems by doping fluorescent dyes into ionic polymers of poly-diallyldimethylammonium bromide (PAB) and poly-diallyldimethylammonium chloride (PAC), where the presence of bromine and chlorine ions provided both structural rigidity and external heavy-atom effects.[59] The rigid polymer PAB can trigger RTP emission among various organic dyes.

Host-guest interaction. Doping emitters into specific host materials can induce excess intermolecular interactions and modulate excited states, as well as avoiding concentration quenching. Naphthalene is a classic aromatic fluorescent dye, which possesses negligible phosphorescence at room temperature. Even by crystallization, the naphthalene still suffers from slow ISC and exciton quenching. Tang et al. employed halogenated benzene as guests doped in naphthalene, successfully induced RTP feature,[60] and the mixture exhibited a τ_P of 760 ms and a Φ_P of 15.6% in 1,4-dichlorobenzene (DCB) host, in which the delocalized molecular orbitals provided new decay path of the triplet excitons, and considerable SOC constants were realized between several singlet and triplet states, facilitating RTP emissions (Fig. 2c). In 2021, Liu et al. reported a unique phenomenon that the carbazole isomer 1*H*-benzo[*f*]indole (Bd) in commercially bought carbazole raw materials could induce strong RTP in some molecules.[61] The trace of Bd inside the (9H-carbazol-9-yl)(4-chlorophenyl)methanone (CphCz) and 4,6-diphenyl-2-carbazolyl-1,3,5-triazine (DphCzT) could trigger the ultra-long RTP emission, where the energy level difference between Bd and carbazole can form charge-separated states under excitation, and radical traps are formed on Bd molecule, and thus elongated exciton recombination time (Fig. 2c). Su et al. doped a series of biphenyl derivatives with different substitutions into benzophenone host, realizing ultra-long RTP emissions.[62] The photoinduced electron transfer (PET) can form an intermediate CT state that can go through efficient ISC process (Fig. 2c). Finally, through energy transfer between the PET state and triplet states of the guests, a high Φ_P of 27.48% with a τ_P of 72.74 ms was realized in the combination of benzophenone (BP) host and 4,4'-bis[*N*-(1-naphthyl)-*N*-phenylamino]biphenyl (NPB) dopant.

Enhancing spin-flip of excitons.

As illustrated in Jablonski diagram, one of the key procedures during phosphorescent emission is spin-flip of excitons. Efficient ISC and radiative decay of triplet excitons are significant to RTP emissions. The ISC can effectively accumulate triplet excitons which determine the upper limit of Φ_P. The ISC rate (k_{ISC}) can be expressed as:[63]

$$k_{ISC} = \frac{2\pi}{\hbar}\left|\langle S|\hat{H}_{SOC}|T\rangle\right|^2 \sqrt{\frac{\pi}{\lambda k_B T}}\, exp\left[-\frac{(\Delta E_{ST}-\lambda)^2}{4\lambda k_B T}\right]$$

thereinto, $\hbar$ denotes the reduced Planck's constant, $\langle S|\hat{H}_{SOC}|T\rangle$ represents SOC matrix between triplet and singlet states, λ is the total reorganization energy, k_B is the Boltzmann constant, T is the temperature, ΔE_{ST} is the energy gap between singlet and triplet states. According to this formula, enhancing SOC matrix constant and reducing ΔE_{ST} are regarded as two important factors to facilitate k_{ISC}.

One important approach towards large SOC is introducing lone-pair electron.[64,65] According to El-Sayed rule, the conservation of angular momentum is pivotal to spin-flip process.[66] The SOC is significantly enhanced between the states with different orbital configurations (e.g., ^{1}n, π* and ^{3}π, π*) compared to the states with similar characters, since the change of angular momentum can be conserved via the change of orbital angular momentum (Fig. 3). The engagements of atoms containing lone-pair electrons (e.g. O, N, S) can modulate the excited state of both singlet or triplet states, providing (n, π*) transition. The SOC matrix constants between (n, π*) and (π, π*) are generally much larger, which are sufficient for ISC process. Practically, the theoretical calculation can evaluate the SOC matrix constants between different states. The SOC matrix constant is structurally dependent, and the optimized molecular structures should be firstly output via commercialized software (e.g. Gaussian, ORCA). After obtaining the optimal structures, the SOC matrix constant can further be calculated by specific software (e.g. ORCA, Dalton). Generally, the same density functional and basis set are consistently employed for both geometry optimization and SOC calculations. Regarding the selection of functionals, an initial screening can be performed based on the molecular structure. Specifically, D–A type RTP emitters dominated by charge transfer transitions prefer functionals with a high Hartree–Fock exchange fraction (e.g., M06-2X, CAM-B3LY P, and wB97X-D). Conversely, conventional RTP emitters dominated by localized excitation may use functionals with a low Hartree–Fock exchange fraction (e.g., B3LYP and PBE0). As for the basis set, the Pople and def2 basis sets are commonly selected. To ensure computational accuracy, the 6-31G**, def2-SVP, or def-TZVP level is typically recommended at least. For molecules containing relatively few atoms, the higher-accuracy def2-TZVP basis set can also be considered. For example, Yuan et al. reported two D–A type molecules, *m*-PBCM and *p*-PBCM, consisting of carbazole and carbonyl groups, which exhibited persistent RTP emissions in sub-seconds scale.[67] The calculated SOC matrix constants between S_1 and T_3 states were 1.97 and 2.18 cm^{-1} for *m*-PBCM and *p*-PBCM, respectively, offering high potential for ISC.

Besides, heave-atom effect is another effective method to augment SOC, as the coupling strength scales with Z^4, where Z represents the nuclear charge of an atom.[68] The commercialized phosphorescent materials contain heavy metals, where the engagement of outer electron orbitals can provide sufficient spin angular momentum. For purely organic emitters, the incorporation of heavy atoms is mainly concentrated on halogens or chalcogens. For instance, He et al. added halogens at the end of the alkyl group of DOPTZ-C3, successfully turning weak RTP emissions into strong RTP emissions.[69]

To maximize k_{ISC}, great efforts have been devoted to narrowing ΔE_{ST}. The traditional aromatic compounds with strong π-conjugation generally possess large exchange energy between S_1 and T_1 states, resulting in large ΔE_{ST}s. The effective pathway for narrowing ΔE_{ST} is introducing donor-acceptor structure to generate ICT state, which can effectively lowering energy gap between S_1 and T_1 states.[70]

Besides k_{ISC}, accelerating phosphorescent decay rate can effectively increase EUE of T_1 excitons and enhance RTP emissions. As evaluated from Einstein coefficient,[71] k_P is related to transition dipole moment between T_1 and S_0 states:

$$k_P = \frac{\Delta E(T_1 - S_0)^3}{3\varepsilon_0 \pi \hbar^4 c^3} \left|\vec{\mu}_{T_1 \to S_0}\right|^2$$

Transition dipole moment $\left|\vec{\mu}_{T_1 \to S_0}\right|^2$ can be expressed as:

$$\vec{\mu}_{T_1 \to S_0} = \sum_n \frac{\langle T_1 | \hat{H}_{SOC} | S_n \rangle}{^3E_1 - {}^1E_n} \times \mu_{S_n - S_0} + \sum_n \frac{\langle T_n | \hat{H}_{SOC} | S_0 \rangle}{^3E_n - {}^1E_0} \times \mu_{T_n - T_1}$$

This expression underscores that SOC matrix constant between singlets-triplet states manifolds is significant for k_P. Meanwhile, increasing transition dipole moment between S_n and S_0 states can also facilitate k_P, as revealed by Hirata.[72]

Overall, the realization of efficient RTP in purely organic systems is a multifaceted challenge that requires the synergistic optimization of both intrinsic molecular electronic structures and extrinsic environmental factors. From a photophysical perspective, enhancing SOC and minimizing ΔE_{ST} remain as the fundamental strategies to facilitate spin-flip processes, thereby effectively populating and utilizing the triplet excitons. Simultaneously, the inherent sensitivity of triplet excitons to oxygen quenching and vibrational deactivation necessitates the meticulous engineering of host matrix or crystalline packing. By providing a rigid microenvironment and modulating intermolecular interactions, these morphological strategies effectively suppress competitive non-radiative decay channels. Ultimately, the strategic balance between accelerating k_P and inhibiting quenching processes is the basement for achieving RTP materials with both high quantum yields and long-lived emission, providing a robust foundation for their application in next-generation optoelectronic devices.

Electroluminescence of RTP emitters

View Article Online
DOI: 10.1039/D6SC03065C

Mechanism of OLEDs. External quantum efficiency (EQE) is a pivotal parameter for evaluating the EL performance of OLEDs, representing the generation efficiency of electrically excited photons. The expression of EQE is described as:[73]

$$EQE = \eta_e \eta_r \chi \Phi_{PL} = \eta_e \times IQE$$

Where η_e is the out-coupling efficiency of an OLED device, η_r represents recombination efficiency of injected carriers, χ is the fraction of radiative excitons, Φ_{PL} is PL quantum yield of emitter. For an emitter used in OLED, Φ_{PL} is a crucial factor that determines the theoretical upper limit of the EQE. According to spin statistics, electrically generated excitons consist of 25% singlets and 75% triplets. The 75% triplet excitons in conventional fluorescent emitters are typically dissipated via non-radiative decay pathways, resulting in an EQE limited to below 5%. For emitters with near unity Φ_{PL}s, the EQE could

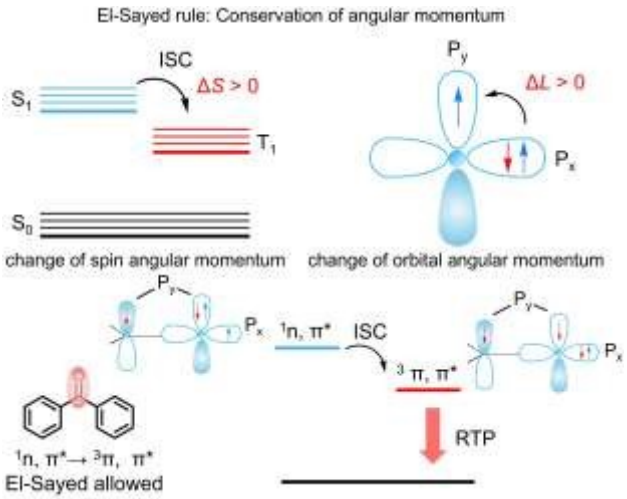

Fig. 3 Schematic diagram of El-Sayed Rule.

reach 25%~30%, in the absence of light-extraction technology. Generally, the efficiency of an OLED device will suffer from a roll-off as the current density increase due to the accumulation of excitons, as the high-concentration excitons will be consumed by non-radiative processes, such as TTA,[47] STA,[74] triplet-polaron annihilation (TPA)[75]. Thus, controlling the exciton lifetimes is a critical method to alleviate exciton loss during EL process. For RTP materials, the inherently long exciton lifetimes of T_1 states are detrimental to OLED applications, thus, a high k_P is preferable for electroluminescent RTP emitters.

Furthermore, sensitization technology which aims to combine the excellent color purity of narrow-spectrum MR-TADF emitters with the high EUE of sensitizers, has emerged as a pivotal strategy in high-definition display.[76,77] Förster resonance energy transfer (FRET) is the key mechanism inside sensitization technology, which possesses the expression:[78]

$$n_{s^* \to A^*} = \frac{9000(ln10)\kappa^2}{128\pi^5 n^4 N \tau_S R^6} \int_0^\infty f_S(\nu) \epsilon_A(\nu) \frac{d\nu}{\nu^4}$$

Thereinto, κ is orientation factor, n is refractive index of environment, N is Avogadro constant, τ_S is prompt decay lifetime of sensitizer, $\int_0^\infty f_S(\nu)\epsilon_A(\nu)\frac{d\nu}{\nu^4}$ is overlap integral between the function of sensitizer's spectrum and absorption of dopant's spectrum. Based on this equation, an ideal sensitizer should possess a high radiative decay rate and an emission spectrum that sufficiently overlaps with the absorption spectrum of the dopant.

Although TADF sensitizers can utilize 100% excitons in principle, the circulation between T_1 and S_1 states may cause long exciton lifetimes and high probability of non-radiative decay as illustrated in Fig. 4a. A radiative T_1 state in RTP emitter can effectively alleviate this problem, where the one-way process during sensitization can consume the excitons rapidly (Fig. 4b).[35,79] During the FRET process from T_1 state to S_1 state, the strong SOC between T_1 and S_0 states of RTP molecules provides the driving force for this spin-flip process of triplet excitons. Thus, purely organic RTP emitters are highly potential as low-cost and high-efficiency sensitizers in OLEDs.

Conventional RTP emitters. The EL of RTP materials has been extensively explored for a long term. Conventional RTP materials are based on simple aromatic compounds with different decorated functional groups, wherein the film morphology and host matrix are significant for phosphorescent emissions. One of the earliest examples of RTP-based OLEDs was reported by Ceroni et al. who synthesized compound **1** which consisted of hexathiobenzene core and peripheral tolyl substituents.[80] The incorporation of sulfur atoms in compound **1** induced the heavy-atom effect, thereby facilitating the ISC process and resulted in prominent phosphorescent emission. Although compound **1** possessed a high Φ_{PL} (80%) in powder, its doped film in polymer hosts exhibited a significantly low Φ_{PL} (2%). The solution-processed OLED based on compound **1** yielded a maximum EQE (EQE_{max}) of 0.1%, indicating poor EUE. Tang et al. synthesized a series of tetra-carbazole phenyl derivatives TCz-F, TCz-H and TCz-OH with different substitutions, exhibiting prominent RTP emissions with long lifetimes of ~2 s.[81] The EL in amorphous films displayed dual-emission characteristics of fluorescence and phosphorescence. The optimal EL performance was achieved by TCz-F, which exhibited an EQE_{max} of 0.29% with commission internationale de l'eclairage (CIE) coordinate of (0.357,0.317), falling within the white emission region. Kim et al. functionalized spiro-fluorene with bromine and carbonyl fluoride to induce heavy-atom effect and (n,π*) transition, respectively, resulting in RTP molecule

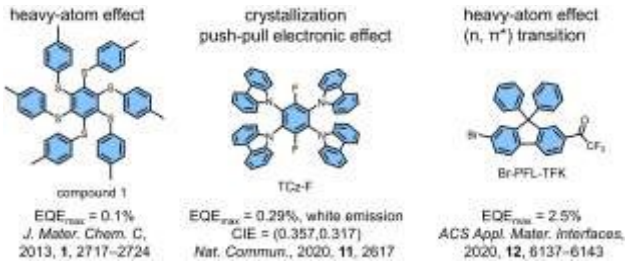

Fig. 5 Molecular structures, mechanisms and corresponding EL performance of the conventional RTP emitters.

BrPFL-TFK.[82] BrPFL-TFK exhibited apparent phosphorescent emission in PMMA matrix, with a Φ_{PL} of 21.2% and a τ_P of 5.28 ms. BrPFL-TFK was doped into three different hosts CBP, mCP and PPT for OLED fabrication. BrPFL-TFK displayed dual emissions in CBP and mCP hosts, consisting of fluorescence and phosphorescence simultaneously, and pure phosphorescent emission was realized only in PPT host. The device employing the PPT host radiated green phosphorescent emissions with an EQE_{max} of 2.5%.

These examples have successfully applied RTP materials in OLEDs, however, the stringent requirements for host selection and device architecture limit their overall EL efficiencies. To compete with other high-efficiency sensitizers such as TADF and organometallic phosphorescence, breakings the limitation of EUE and host selection is critical for RTP emitters.

D–A type RTP emitters and sensitizers. After the rapid development of TADF materials, the construction of ICT has emerged as a vital strategy for modulating excited states. ICT effectively reduces the exchange energy between S_1 and T_1 states, resulting in small ΔE_{ST}s. The general approach of ICT is adopting D–A structures into molecular skeletons, which can separate the highest occupied molecular orbital (HOMO) and the lowest unoccupied molecular orbital (LUMO). The separation of spatial distribution of HOMO and LUMO can also modulate the SOC between triplet and singlet states, accelerating both ISC and k_P. For such kind of D–A type RTP emitters, the host dependence is weakened as compared to those conventional RTP emitters lacking ICT characteristic, and the main consideration concerns on the matching of triplet energy level and carrier transportability. Generally, carbazole-based host materials are preferred for these D–A type RTP emitters, due to their high T_1 energy level and good carrier transportability.[83] Additionally, phosphine oxide-based hosts featuring high T_1 energy levels and sterically crowded structures have also been applied for RTP emitters, as they can effectively restrict molecular motions via intermolecular hydrogen bonds and mitigate intermolecular interactions.[84] The EL performance of representative RTP-based OLEDs and RTP-sensitized OLEDs are summarized in Table 1 and Table 2.

Recently, Wang et al. integrated a sulfur-containing phenothiazine donor into naphthalene core, realizing an orange-emitting RTP molecule DPTZN.[85] Theoretical calculations revealed that DPTZN possessed two isomeric configurations. The *cis*-DPTZN whose natural transition orbital (NTO) of $T_1 \rightarrow S_0$ was featured as CT characteristic possessed a large SOC matrix constant of 1.28 cm^{-1}, while *trans*-DPTZN featured as locally excited characteristic exhibited nearly zero SOC matrix constant. By doping DPTZN into TRZ-BIM host, a good EQE_{max} of 11.5% was realized, with CIE coordinate of (0.46, 0.52). Lee et al. designed RTP materials via similar strategy by selecting phenoselenazine containing a selenium atom as electron donor.[86] Three molecules PSe1, PSe2 and PSe3 were synthesized where phenoselenazine was connected to phenyl or biphenyl group in different positions. The EQE_{max}s of PSe1,

View Article Online
DOI: 10.1039/D6SC03065C

Table 1. EL performances of RTP-based OLEDs.[a]

Emitter	τ_P	Φ_{PL} (%)	λ_{EL} (nm)	EQE_{max} (%)	Ref
Compound 1	3.0μs	80	485	0.1	80
TCz-F	520 ms	0.8	420, 580	0.29	81
Br-PFL-TFK	23.8 ms	24.0	~518	2.5	82
DPTZN	87μs	38	~570	11.5	85
PSe1	0.61ms	0.33	523	10.7	86
PSe2	0.64ms	0.35	523	10.0	86
PSe3	0.93ms	0.27	523	8.1	86
P(DMPAc-O-TPTrz)	1642.6 ns	49.5	495	9.7	87
P(DMPAc-O-TPOD)	12.67 ms	16.5	510	3.7	89
D32	763.0 ns	29.2	504	6.7	90
bTEoCN	15.2 ms	37.0	590	8.7	93
bTENCO	12.9 ms	68.0	~540	18.9	93
bTEpCN	–	99.9	~548	25.1	93
PXSeDRZ	1.21 ms	68.1	550	19.5	91
BPXSeDRZ	2.1 ms	66.3	554	17.2	92
DBPXSeDRZ	1.7 ms	66.9	567	17.9	92
XT-DPA	–	46.0	456	6.6	99
XT-*t*DPA	–	56.0	470	18.6	99
TXT-DPA	450.3μs	72.0	474	17.7	99
TXT-*t*DPA	126.4μs	93.0	486	27.3	99
2,3-PICz-XT	8.1μs	92.0	508	32.7	100
3,2-PICz-XT	2.9μs	72.0	522	24.9	101
3,2-PICz-TXT	1.4μs	97.0	508	33.2	36

[a]Abbreviations: τ_P = phosphorescent lifetimes of emitters in films. Φ_{PL} = photoluminescence quantum yields of emitters in films. λ_{EL} = EL peak of OLED. EQE_{max} = maximum external quantum efficiency of OLED.

PSe2 and PSe3 were 10.7%, 10.0% and 8.1%, respectively, where the high exciton utilization could be attributed to heavy-atom effect of selenium.

In 2020, Ding et al. designed a RTP polymer P(DMPAc-O-TPTrz) where the monomer was constructed by a D–O–A structure.[87] The oxygen bridge could weaken the overlap between HOMO and LUMO, suppressing the CT fluorescence. The oxygen bridge also endowed the monomer with enhanced SOC, which facilitated the spin-flip process from singlet to triplet state. The resulting polymer-based OLED displayed a high EQE_{max} of 9.7%. Besides, P(DMPAc-O-TPTrz) was also used as sensitizer for an orange emitter TBRB, yielding white emission with an EQE_{max} of 7.4% and CIE coordinate of (0.30, 0.43).[88] Inspired by this phenomenon, Ding et al. substituted triazine acceptor with dibenzothiophene-S,S-dioxide,[89] realizing white emission polymer P(DMPAc-O-DBTDO). By adjusting doping concentration of P(DMPAc-O-DBTDO), correlated color temperatures were ranged from 4834 to 6741 K, with high color rendering index above 65. An EQE_{max} of 3.7% was obtained at the doping concentration of 20 wt%, with Commission Internationale de l'Eclairage (CIE) coordinate of (0.30, 0.44). The benzophenone acceptor was further introduced to this D–O–A structure, and a small molecule RTP emitter D32 was obtained.[90] D32 possessed an EQE_{max} of 6.70% in OLED, exhibiting cyan phosphorescence. D32 was also utilized as sensitizer for MR-TADF emitter S-CZ-BN, realizing a narrow-spectrum emission peaking at 490 nm, with an EQE_{max} of 17.11%.

Su et al. also contributed numerous high-efficiency RTP materials for OLEDs. The selenium contained electron donor phenoxaselenine was connected to three different acceptors 2DPm, 4DPm and DRZ, resulting in three D–A type molecules PXSe2DPm, PXSe4DPm and PXSe2DRZ.[91] The DRZ acceptor could not only establish intramolecular confinement through hydrogen bonds but also endowed PXSe with a folded configuration. The lone-pair electrons in selenium atom were not parallel to the orbitals on DRZ acceptor, providing excess angular momentum change for spin-flip of excitons. The OLEDs based on PXSe2DPm, PXSe4DPm and PXSe2DRZ exhibited EQE_{max}s of 7.3%, 16.0% and 19.5%, respectively. Thereinto, PXSe2DRZ demonstrated pure phosphorescent emission and comparable EL efficiencies to those of metallic phosphors. By extending PXSe with naphthalene and phenanthrene which contain large π-conjugations, the resulted molecules BPXSeDRZ and DBPSeDRZ possessed red-shifted RTP emissions.[92] BPXSeDRZ and DBPSeDRZ also performed well in OLEDs where the EQE_{max} reached 17.2% and 17.9%, respectively. Moreover, DBPSeDRZ was adopted as sensitizer for a red conventional fluorescent emitter DBP, realizing an EQE_{max} of 10.1% with CIE coordinate of (0.61, 0.38). Besides, rigid polycyclic RTP emitters were also developed by the same group.[93] The sulfur bridged molecular skeletons displayed different photophysical properties by alternating bridged position, where the pure RTP, combined RTP and TADF, pure TADF properties could be adjusted through molecular engineering. The pentaphene-based molecule bTEoCN possessed a folded structure and exhibited pure RTP emission, while the pentacene-based molecule bTEpCN with a symmetric structure somehow showed TADF property. The bTENCO which integrated an imide in bTEoCN skeleton displayed a dual emission containing RTP and

View Article Online
DOI: 10.1039/D6SC03065C

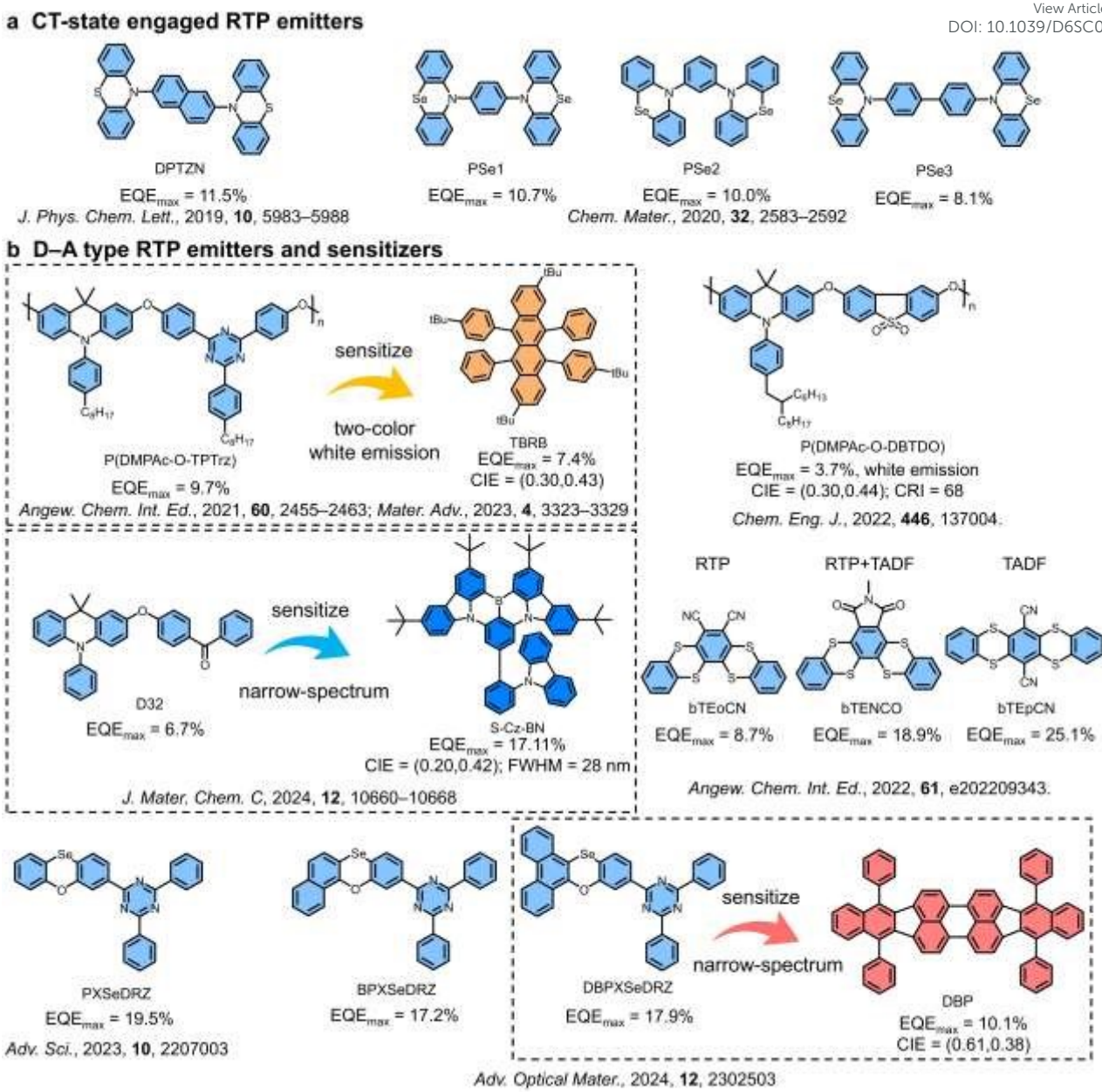

Fig. 6 Molecular structures and corresponding EL performance of (a) CT-state engaged and (b) D–A type RTP emitters and sensitizers. The molecules inside box represent the pair of sensitizers and dopants.

TADF (Fig. 6b). The OLEDs based on bTEoCN, bTENCO and bTEpCN showed the EQE$_{max}$s of 8.7%, 18.9% and 25.1%, respectively. The spectrum of bTEoCN was composed of both fluorescence and phosphorescence, while the pure TADF emission was observed for bTEpCN. This work discovered the RTP phenomenon in polycyclic aromatic rings, bringing about new guidance for realizing high-efficiency purely organic phosphors.

Carbonyl-based RTP emitters and sensitizers. Although RTP-based OLEDs have been extensively researched, their application as purely organic sensitizers is a quite recent development. The relatively low efficiency of the early developed RTP materials makes them inappropriate for sensitizers. Moreover, some of the RTP molecules containing halogens or hydroxy may bring about negative effect on device stability.

Carbonyl group is a classical electron acceptor characterized by lone-pair electrons, which can facilitate (n, π*) transitions in organic molecules. Several D–A type TADF emitters containing carbonyl group have been developed, which can realize high efficiency and impressive stability. In past few years, we have comprehensively studied the organic luminescent materials based on carbonyl-containing acceptors,[19,32,64,94-98] and found that the distinct (n, π*) transition enhances the SOC between the singlet and triplet manifolds, while concentration quenching is suppressed by the large steric hindrance of carbonyl acceptors (benzophenone, xanthone, acridone, etc.). Very

View Article Online
DOI: 10.1039/D5SC03065C

Table 2. EL performance of RTP-sensitized OLEDs.[a]

Sensitizer	Dopant	λ_{EL} (nm)	FWHM (nm)	CIE (x,y)	EQE_{max} (%)	Ref
P(DMPAc-O-TPTrz)	TBRB[b]	–	–	(0.30,0.43)	7.4	86
D32	S-Cz-BN[c]	490	18	(0.20,0.42)	17.11	88
DBPXSeDRZ	DBP[c]	610	~23	(0.61,0.38)	10.1	90
2,3-PICz-XT	BN2[c]	540	42	(0.314, 0.639)	35.02	98
	BN3[c]	564	41	(0.439, 0.539)	35.13	
	PO-01-TB	556	–	(0.474, 0.513)	37.26	
	4CzTPNBu	556	–	(0.454, 0.515)	31.84	
	$Ir(MDQ)_2acac$	598	–	(0.554, 0.403)	29.65	
	$Ir(piq)_2acac$	620	–	(0.643, 0.330)	26.81	
	TPA-AQ	594	–	(0.478, 0.426)	30.10	
3,2-PICz-TXT	BN2[c]	540	40	(0.32.0.65)	43.8	36
	tCzphB-Fl[c]	538	31	(0.29.0.68)	43.8	
	tCzphB-Ph[c]	526	30	(0.23,0.71)	40.9	

[a]Abbreviations:. λ_{EL} = EL peak of OLED. FWHM = full-width at half-maximum of spectrum. CIE = commission internationale de l'eclairage coordinates. EQE_{max} = maximum external quantum efficiency of OLED. [b]The resulted device is a white-emission OLED, where the spectrum is composed of multiple peaks. [c]These dopants are featured as narrow-spectrum emissions.

recently, we discovered RTP phenomena in the carbonyl-based emitters, establishing a new set of robust sensitizers.

In former perspective, constructing rigid molecular skeleton can reduce the non-radiative decay of triplet excitons, facilitating RTP emissions. Two flexible electron donors diphenylamine (DPA) and *tert*-butyl-diphenylamine (*t*DPA) are introduced into carbonyl-based electron acceptor of xanthone (XT) or thioxanthone (TXT), generating four luminescent molecules XT-DPA, XT-*t*DPA, TXT-DPA and TXT-*t*DPA (Fig. 7d).[99] The XT-based molecules XT-DPA and XT-*t*DPA displayed TADF emission but no phosphorescent emission at room temperature. In contrast, TXT-DPA and TXT-*t*DPA exhibited dual channel emissions of TADF and RTP phenomena, owing to the heavy-atom effect from sulfur atom in TXT. The doped OLEDs based on XT-DPA and XT-*t*DPA possessed EQE_{max}s of 6.6% and 18.6% respectively, inferior to TXT-DPA (17.7%) and TXT-*t*DPA (27.3%). The EL differences between XT and TXT emitters demonstrate the critical role of heavy-atom effect, and the presence phosphorescent decay path could increase the EUE of OLEDs.

Indolocarbazole isomers with rigid skeleton and large π-conjugated planes are widely used electron donors. Two 11-phenylindolo[2,3-a]carbazole (2,3-PICz) connected to XT acceptor resulted in a D–A–D type molecule 2,3-PICz-XT which can open up the radiative path of triplet excitons.[100] Large SOC matrix constants between S_1 and T_1, T_2, and T_3 states were proved by theoretical calculations, which contributed to the engagement of (n, π*) transition. The phosphorescent emission was confirmed by bubbling oxygen into toluene solutions, where the prominent blue shifted and weakened emission spectrum was observed. The PL spectrum measured at 1 ms delay also exhibited pronounced red shifts. By the comprehensive analysis from experimental data, it was confirmed that 2,3-PICz-XT showed dual-emission characteristic of both fluorescence and phosphorescence. The OLEDs employed 2,3-PICz-XT as emitter exhibited the highest EQE_{max} of 32.73% at the doping concentration of 20 wt% in PPF host, peaking at 508 nm. Furthermore, 2,3-PICz-XT was adopted as sensitizer for metallic phosphorescent emitter, TADF emitter and MR-TADF emitter, exhibiting impressive EQE_{max}s ranging from 26.81% to 37.26% (Fig. 7a). Notably, the red emitter $Ir(MDQ)_2acac$ and TPA-AQ achieved remarkably high EQE_{max}s of 29.65% and 30.10%, respectively, representing one of the highest EL efficiencies reported for these emitters. The core mechanism is that the delayed fluorescence and phosphorescence can sensitize dopants through FRET simultaneously, realizing multi-channel sensitization.

Through the isomeric strategy of electron donor, 3,2-PICz-XT was synthesized, which possessed the phosphorescent quantum yield (Φ_P) and fluorescent quantum yield (Φ_F) of 30% and 42%, respectively (Fig. 7b).[101] The k_P of 3,2-PICz-XT was 1.03×10^5 s^{-1}, remarkably faster than those of generally reported purely organic RTP molecules. The non-doped OLEDs based on 3,2-PICz-XT displayed a high EQE_{max} of 24.91%, with negligible roll-off at 1000 cd m^{-2}. 3,2-PICz-XT was further applied in a simplified ultra-thick OLED, where the EML was 80 nm, and a high EQE_{max} of 17.79% was obtained. The non-doped OLED based on 3,2-PICz-XT is prominently better than those based on carbonyl-based RTP emitters with DPA or *t*DPA donors. Such improvement of non-doped OLEDs is mainly attributed to the rigidified molecular structures, which stabilized triplet excitons and facilitated carrier transport in amorphous film.

To further increase the SOC matrix constants, the 3,2-PICz-TXT with TXT acceptor was `designed and synthesized (Fig. 7c).[36] The purely organic RTP emitter 3,2-PICz-TXT owned a high phosphorescence ratio of 98.3%, with a fast k_P of 6.8×10^5 s^{-1}. The OLED utilized 3,2-PICz-TXT as emitter depicted an outstanding EQE_{max} of 33.2%, which exceeded a commercial metallic phosphorescent emitter $Ir(ppy)_3$ (25.2%) under the same device structure. By employing 3,2-PICz-TXT as sensitizer, three MR-TADF dopants BN2, tCzphB-Fl and tCzphB-Ph realized ultrahigh EQE_{max}s of 43.8%, 43.3% and 40.9%, respectively. More impressively, the power efficiencies of the devices based

View Article Online
DOI: 10.1039/D6SC03065C

on BN2 and tCzphB-Fl were even close to 200 lm W^{-1}. These devices represent the state-of-the-art narrow-spectrum OLEDs. Besides, the operational lifetime can also be enhanced by this RTP sensitizer, where the LT_{80} lifetime (the time when the luminance decays to 80% of the initial luminance) of tCzphB-Fl can be raised from 15.0 to 110.1 h under the sensitization of 3,2-PICz-TXT.

Notably, the horizontal dipole ratios of 2,3-PICz-XT and 3,2-PICz-XT are as high as 82.7% and 78.0%, respectively. The D–A structure can effectively enhance intramolecular polarity,

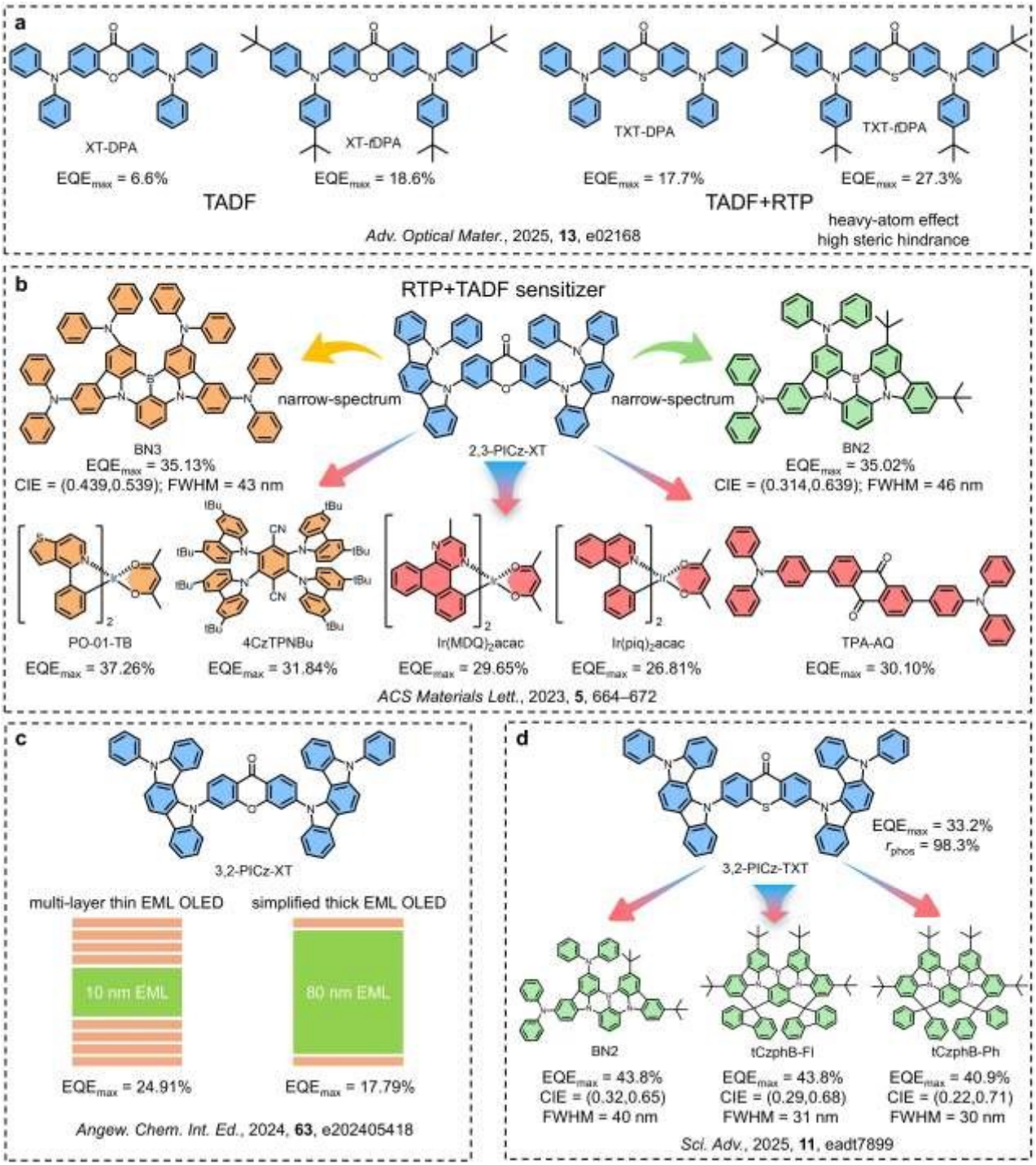

Fig. 7 (a) Molecular structures and EL efficiencies of TADF and RTP emitters XT-DPA, XT-*t*DPA, TXT-DPA and TXT-*t*DPA. (b) Summary of RTP and TADF dual-emission sensitizer 2,3-PICz-XT and dopants. BN2 and BN3 are narrow-spectrum MR-TADF emitters; PO-01-TB, Ir(MDQ)$_2$acac and Ir(piq)$_2$acac are metallic phosphorescent emitters; 4CzTPNBu and TPA-AQ are TADF emitters. (c) Summary of RTP emitter 3,2-PICz-XT, the OLEDs are based on non-doped films. (d) Summary of RTP sensitizer 3,2-PICz-TXT. BN2, tCzphB-Fl and tCzphB-Ph are narrow-spectrum MR-TADF emitters.

facilitating orientation polarization.[102] Meanwhile, the rigid and highly planar PICz donors expand molecular planes where the transition dipole moment lies. These carbonyl-based RTP emitters are instructive examples for designing horizontally oriented molecules.

Conclusion and outlook

Significant efforts have been devoted to the molecular design and OLED applications of RTP emitters and sensitizers. In this perspective, the design principles of RTP emitters which have been thoroughly explored in past few decades are briefly summarized. More importantly, the significance of developing RTP sensitizers is emphasized, as they are pivotal for next-generation OLED displays. The one-way decay characteristic of RTP sensitizers can resolve exciton cycling issues thereby achieving high efficiency and stability. The D–A skeleton is an ideal molecular design strategy for high efficiency RTP sensitizers, where the incorporation of lone-pair electrons and heavy atoms are also necessary. Practically applicable RTP sensitizers based on carbonyl-containing XT and TXT acceptors can be prospectively developed through synergistic molecular design strategies.

The core issue concerning RTP sensitizers remains their lack of stability. To alleviate the triplet exciton quenching, the rate constant k_{ISC} and k_P should be further increased, which would reduce the lifetime of the triplet excitons. Meanwhile, proper heavy atoms should be carefully selected during molecular design, since their introduction may weaken the chemical bonding energies. Besides, efficient blue RTP emitters are still rare. The realization of blue emissions in organic emitters is highly dependent on shortening π-conjugation length or weakening ICT effect, which restrict the structural multiplicity of the emitters. Although a few studies have successfully developed blue RTP emitters,[104-106] their reliance on specific rigid polymer host matrices limits their practical application in OLEDs. In that case, the development of high-performance blue RTP-OLEDs still demands substantial research efforts. Furthermore, compatible functional materials (e.g. host and blocking materials) should be further developed to maximize the performance of RTP materials.

Author contributions

Z. Zhao conceived the project. H. Liu and Y. Fu organized and wrote the paper. Z. Zhao revised the paper. Z. Zhao, B. Z. Tang and J. W. Y. Lam supervised the project.

Conflicts of interest

The authors declare no conflict of interest.

Acknowledgements

This work is financially supported by the National Natural Science Foundation of China (U23A20594 and 22375066), the GuangDong Basic and Applied Basic Research Foundation (2023B1515040003), the Innovation and Technology Commission (ITC-CNERC14SC01) and the Postdoctoral Fellowship Program and China Postdoctoral Science Foundation (BX20250109).

Notes and references

1 C. W. Tang and S. A. Vanslyke, *Appl. Phys. Lett.*, 1987, **51**, 913–915.
2 J. H. Burroughes, D. D. C. Bradley, A. R. Brown, R. N. Marks, K. Mackay, R. H. Friend, P. L. Burns and A. B. Holmes, *Nature*, 1990, **347**, 539–541.
3 S. Liu, L. Lan and H. Zhang, *Chem. Sci.*, 2025, **16**, 18919–18927.
4 W. Feng, X. Liao, S. Lu, D. Han, Q. Guo, Y. Zhao, W. Tian and H. Yan, *Chem. Sci.*, 2025, **16**, 22517–22526.
5 B. Zhang, X. Shao, W. Yin, J. Xu, B. Wu, Z. An and H. Shi, *FlexMat*, 2026, 1–13. https://doi.org/10.1002/flm2.70049
6 J. Liang, B. Z. Tang and B. Liu, *Chem. Soc. Rev.*, 2015, **44**, 2798-2811.
7 J. Li, J. Gu, L. Ding, X. Li, P. Xia, F. Liu, X. Chen, W. Ma, Y. He, Q. Li, Z. Li, and Y. Yuan, *Aggregate*, 2025, **6**, e70031.
8 L. J. Rothberg and A. J. Lovinger, *J. Mater. Res.*, 1996, **11**, 3174–318.
9 Y. Ma, H. Zhang and C. Che, *Synth. Met.*, 1998, **94**, 245–248.
10 M. A. Baldo, D. F. O'Brien, Y. You, A. Shoustikov, S. Sibley, M. E. Thompson and S. R. Forrest, *Nature*, 1998, **395**, 151–154.
11 G. Li, Q. Chu, H. Yao, K. Wu and Y.-B. She, *Nat. Photonics*, 2025, **19**, 977–984.
12 D. N. Tritton, F.-K. Tang, G. B. Bodedla, F.-W. Lee, C.-S. Kwan, K. C.-F. Leung, X. Zhu and W.-Y. Wong, *Coord. Chem. Rev.*, 2022, **459**, 214390.
13 D. Zhang, H. Dai, H. Zhang and L. Duan, *Nat. Photonics*, 2026, **20**, 136–150.
14 Z. Zhou, H. Wang, J. Yao, T. Wang, J. Liu, X. Cao, Q. Feng, B. Yue, D. Wang, J. Wang and H. Huang, *Aggregate*, 2026, **3**, e70296.
15 H. Uoyama, K. Goushi, K. Shizu, H. Nomura and C. Adachi, *Nature*, 2012, **492**, 234–238.
16 W. Li, Y. Pan, R. Xiao, Q. Peng, S. Zhang, D. Ma, F. Li, F. Shen, Y. Wang, B. Yang and Y. Ma, *Adv. Funct. Mater.*, 2014, **24**, 1609–1614.
17 X. Ai, E. W. Evans, S. Dong, A. J. Gillett, H. Guo, Y. Chen, T. J. H. Hele, R. H. Friend and F. Li, *Nature*, 2018, **563**, 536–540.
18 Q. Zhang, B. Li, S. Huang, H. Nomura, H. Tanaka and C. Adachi, *Nat. Photonics*, 2014, **8**, 326–332.
19 Y. Fu, H. Liu, B. Z. Tang and Z. Zhao, *Nat. Commun.*, 2023, **14**, 2019.
20 Y. Chen, D. Zhang, Y. Zhang, X. Zeng, T. Huang, Z. Liu, G. Li and L. Duan, *Adv. Mater.*, 2021, **33**, 2103293.
21 R.-Z. An, F.-M. Zhao, C. Shang, M. Zhou and L.-S. Cui, *Angew. Chem. Int. Ed.*, 2025, **64**, e202420489.
22 D. Liu, G.-X. Yang, Z. Chen, W. Xie, D. Li, W. Li, J. Lin, X. Nie, Z. Li, B. Liang, Z. Yang, Z. Wang, J. Pu, G. Sun, C. Shen, M. Li and S.-J. Su, *Adv. Mater.*, 2024, **36**, 2403584.
23 Y. Kondo, K. Yoshiura, S. Kitera, H. Nishi, S. Oda, H. Gotoh, Y. Sasada, M. Yanai and T. Hatakeyama, *Nat. Photonics*, 2019, **13**, 678–682.
24 T. Huang, Y. Xu, Y. Qu, X. Lu, K. Ye, X. Zhuang and Y. Wang, *Adv. Mater.*, 2025, **37**, 2503383.
25 X. Qiu, G. Tian, C. Lin, Y. Pan, X. Ye, B. Wang, D. Ma, D. Hu, Y. Luo and Y. Ma, *Adv. Opt. Mater.*, 2021, **9**, 2001845.
26 X. Wang, L. Wang, G. Meng, X. Zeng, D. Zhang and L. Duan, *Sci. Adv.*, 2023, **9**, eadh1434.
27 T. Hua, X. Cao, J. Miao, X. Yin, Z. Chen, Z. Huang and C. Yang, *Nat. Photonics*, 2024, **18**, 1161–1169.

28 C. Qu, Y. Wu, L. Duan and Y. Zhang, *Angew. Chem. Int. Ed.,* 2026, **65**, e3968771.
29 X. Wu, S. Ni, C.-H. Wang, W. Zhu, P.-T. Chou, *Chem. Rev.,* 2025, **125**, 6685–6752.
30 C.-Y. Chan, M. Tanaka, Y.-T. Lee, Y.-W. Wong, H. Nakanotani, T. Hatakeyama and C. Adachi, *Nat. Photonics*, 2021, **15**, 203–207.
31 T. Huang, Q. Wang, H. Zhang, Y. Zhang, G. Zhan, D. Zhang and L. Duan, *Nat. Photonics*, 2024, **18**, 516–523.
32 H. Liu, Y. Fu, J. Zhang, X. Dong, N. Zheng, D. Yang, X. Qiao, D. Ma, J. Sun, J. W. Y. Lam, B. Z. Tang and Z. Zhao, *Angew. chem. Int. Ed.*, 2025, **64**, e202511525.
33 J. Yan, D. Y. Zhou, L. S. Liao, M. Kuhn, X. Zhou, S. M. Yiu and Y. Chi, *Nat. Commun.*, 2023, **14**, 6419.
34 R. Tang, S. Xu, G. Cheng, K.-H. Low, D. Zhang, L. Duan, C.-M. Che, *Nat. Commun.* 2025, **16**, 7776.
35 C. Yin, Y. Xin, T. Huang, Q. Zhang, L. Duan and D. Zhang, *Nat. Commun.*, 2025, **16**, 30.
36 J. Zeng, S. Song, Y. Fu, X. Peng, B. Z. Tang and Z. Zhao, *Sci. Adv.*, 2025, **11**, 7899.
37 J. Lou, L. Xu, W. Ju, D. Wang, T. Cheng, W. Zhu, N. Su and J. Ding, *J. Mater. Chem. C*, 2024, **12**, 10660–10668.
38 W. Zhao, Z. He and B. Z. Tang, *Nat. Rev. Mater.*, 2020, **5**, 869–885.
39 Z. Yin, Q. Sun, Z. Wu, Y. Xu, Z. Xie, and B. Liu, *Aggregate*, 2025, **6**, e70141.
40 M. Li, Z. Chen, K. Liu, Q. He and S.-J. Su, *FlexMat*, 2025, **2**, 145.
41 W. Z. Yuan, X. Y. Shen, H. Zhao, J. W. Y. Lam, L. Tang, P. Lu, C. Wang, Y. Liu, Z. Wang, Q. Zheng, J. Z. Sun, Y. Ma and B. Z. Tang, *J. Phys. Chem. C*, 2010, **114**, 6090–6099.
42 N. Aizawa, Y. J. Pu, M. Watanabe, T. Chiba, K. Ideta, N. Toyota, M. Igarashi, Y. Suzuri, H. Sasabe and J. Kido, *Nat. Commun.*, 2014, **5**, 5756.
43 M. Inoue, N. Oyabu, Y. Kaneko, J.-Y. Kim, J.-H. Yang, *J. Soc. Inf. Display.* 2020, **28**, 905–910.
44 D. Chaudhuri, E. Sigmund, A. Meyer, L. Röck, P. Klemm, S. Lautenschlager, A. Schmid, S. R. Yost, T. Van Voorhis, S. Bange, S. Höger and J. M. Lupton, *Angew. chem. Int. Ed.*, 2013, **52** , 13449–13452.
45 A. Krishna, V. Darshan, C. H. Suresh, K. N. Narayanan Unni and R. L. Varma, *J. Photochem. Photobiol., A*, 2018, **360**, 249–254.
46 C. Li, M. Wu, Z. Zhao, J. W. Y. Lam, B. Xu and B. Z. Tang, *Chem*, 2025, **11**, 102654.
47 W. Staroske, M. Pfeiffer, K. Leo and M. Hoffmann, *Phys. Rev. Lett.*, 2007, **98**, 197402.
48 F. Wilkinson and A. A. Abdel-Shafi, *J. Phys. Chem. A*, 1997, **101**, 5509–5516.
49 G. C. Smith, *Phys. Rev.*, 1968, **166**, 839.
50 K. P. Ghiggino, C. H. Nicholls and M. T. Pailthorpe, *Photochem. Photobiol.*, 1975, **22**, 169–173.
51 D. Levy and D. Avnir, *J. Photochem. Photobiol., A*, 1991, **57**, 41.
52 L. Gu, H. Shi, L. Bian, M. Gu, K. Ling, X. Wang, H. Ma, S. Cai, W. Ning, L. Fu, H. Wang, S. Wang, Y. Gao, W. Yao, F. Huo, Y. Tao, Z. An, X. Liu and W. Huang, *Nat. Photonics*, 2019, **13**, 406–411.
53 H. Y. Gao, Q. J. Shen, X. R. Zhao, X. Q. Yan, X. Pang and W. J. Jin, *J. Mater. Chem.*, 2012, **22**, 5336–5343.
54 D. Lee, O. Bolton, B. C. Kim, J. H. Youk, S. Takayama and J. Kim, *J. Am. Chem. Soc.*, 2013, **135**, 6325–6329.
55 W. Gao, Y. Su, Z. Wang, Y. Zhang, D. Zhang, P. Jia, C. Yang, Y. Li, R. Ganguly and Y. Zhao, *ACS Appl. Mater. Interfaces*, 2019, **11**, 47162–47169.
56 M. S. Kwon, D. Lee, S. Seo, J. Jung and J. Kim, *Angew. chem. Int. Ed.*, 2014, **53**, 11177–11181.
57 Q. Yao, Z. Wang, A. Allam, Z. Da, C. Zhang, J. Wang and M. Wang, *J. Mater. Chem. C*, 2025, **13**, 12754–12761.
58 D.-X. Ma, Z.-Q. Li, K. Tang, Z.-L. Gong, J.-Y. Shao and Y.-W. Zhong, *Nat. Commun.*, 2024, **15**, 4402.
59 Z.-A. Yan, X. Lin, S. Sun, X. Ma and H. Tian, *Angew. chem. Int. Ed.*, 2021, **60**, 19735–19739.
60 X. Zhang, J. Liu, B. Chen, X. He, X. Li, P. Wei, P. F. Gao, G. Zhang, J. W. Y. Lam and B. Z. Tang, *Matter*, 2022, **5**, 3499–3512.
61 C. Chen, Z. Chi, K. C. Chong, A. S. Batsanov, Z. Yang, Z. Mao, Z. Yang and B. Liu, *Nat. Mater.*, 2021, **20**, 175–180.
62 W. Qiu, X. Cai, M. Li, Z. Chen, L. Wang, W. Xie, K. Liu, M. Liu and S.-J. Su, *J. Phys. Chem. Lett.*, 2021, **12**, 4600–4608.
63 G. Baryshnikov, B. Minaev and H. Ågren, *Chem. Rev.*, 2017, **117**, 6500–6537.
64 Y. Fu, H. Liu, D. Yang, D. Ma, Z. Zhao and B. Tang, *Adv. Opt. Mater.*, 2022, **10**, 2102339.
65 R. Walia, X. Fan, L. Mei, W. Guo, K. Wang, C. Adachi, X.-K. Chen and X.-H. Zhang, *Angew. chem. Int. Ed.,* 2025, **64**, e202503371.
66 M. A. El-Sayed, *Acc. Chem. Res.* 1968, **1**, 8–16.
67 Z. He, H. Gao, S. Zhang, S. Zheng, Y. Wang, Z. Zhao, D. Ding, B. Yang, Y. Zhang and W. Z. Yuan, *Adv. Mater.*, 2019, **31**, 1807222.
68 B. Minaev, G. Baryshnikov and H. Agren, *Phys. Chem. Chem. Phys.*, 2014, **16**, 1719.
69 H. Li, H. Ma, P. Zhang, Z. An and X. He, *Angew. chem. Int. Ed.*, 2025, **64**, e202419366.
70 D. Veldman, S. C. J. Meskers and R. A. J. Janssen, *Adv. Funct. Mater.*, 2009, **19**, 1939–1948.
71 K. Schmidt, S. Brovelli, V. Coropceanu, D. Beljonne, J. Cornil, C. Bazzini, T. Caronna, R. Tubino, F. Meinardi, Z. Shuai and J. L. Brédas, *J. Phys. Chem. A*, 2007, **111**, 10490–10499.
72 S. Hirata, *J. Phys. Chem. Lett.*, 2018, **9**, 4251–4259.
73 Z. Wu and D. Ma, *Mater. Sci. Eng., R*, 2016, **107**, 1–42.
74 C. Lin, P. Han, F. Qu, S. Xiao, Y. Li, D. Xie, X. Qiao, D. Yang, Y. Dai, Q. Sun, A. Qin, B. Z. Tang and D. Ma, *Mater. Horiz.*, 2022, **9**, 2376–2383.
75 M. Hasan, S. Saggar, A. Shukla, F. Bencheikh, J. Sobus, S. K. M. McGregor, C. Adachi, S.-C. Lo and E. B. Namdas, *Nat. Commun.*, 2022, **13**, 254.
76 H. Nakanotani, T. Higuchi, T. Furukawa, K. Masui, K. Morimoto, M. Numata, H. Tanaka, Y. Sagara, T. Yasuda and C. Adachi, *Nat. Commun.*, 2014, **5**, 4016.
77 D. Zhang, L. Duan, C. Li, Y. Li, H. Li, D. Zhang and Y. Qiu, *Adv. Mater.*, 2014, **26**, 5050–5055.
78 T. Főrster, 10th Spiers Memorial Lecture. Transfer Mechanisms of Electronic Excitation, *Discuss. Faraday Soc.*, 1959, **27**, 7–17.
79 C. Yin, Y. Zhang, T. Huang, Z. Liu, L. Duan and D. Zhang, *Sci. Adv.*, 2022, **8**, eabp9203.
80 G. Bergamini, A. Fermi, C. Botta, U. Giovanella, S. D. Motta, F. Negri, R. Peresutti, M. Gingras and P. Ceroni, *J. Mater. Chem. C*, 2013, **1**, 2717–2724.
81 H.-T. Feng, J. Zeng, P.-A. Yin, X.-D. Wang, Q. Peng, Z. Zhao, J. W. Y. Lam and B. Z. Tang, *Nat. Commun.*, 2020, **11**, 2617.
82 B. Song, W. Shao, J. Jung, S. J. Yoon and J. Kim, *ACS Appl. Mater. Interfaces*, 2020, **12**, 6137–6143.
83 B. Wex and B. R. Kaafarani, *J. Mater. Chem. C*, 2017, 5, 8622–8653
84 J. Li, D. Ding, Y. Tao, Y. Wei, R. Chen, L. Xie, W. Huang and H. Xu, *Adv. Mater.*, 2016, **28**, 3122—3130
85 J. Wang, J. Liang, Y. Xu, B. Liang, J. Wei, C. Li, X. Mu, K. Ye and Y. Wang, *J. Phys. Chem. Lett.*, 2019, **10**, 5983–5988.
86 D. R. Lee, K. H. Lee, W. Shao, C. L. Kim, J. Kim and J. Y. Lee, *Chem. Mater.*, 2020, **32**, 2583–2592.
87 X. Liu, L. Yang, X. Li, L. Zhao, S. Wang, Z. H. Lu, J. Ding and L. Wang, *Angew. chem. Int. Ed.*, 2021, **60**, 2455–2463.
88 Y. Tian, R. He, G. Meng, S. Wang, L. Zhao and J. Ding, *Mater. Adv.*, 2023, **4**, 3323–3329.
89 D. Mei, L. Yan, X. Liu, L. Zhao, S. Wang, H. Tian, J. Ding and L. Wang, *Chem. Eng. J.*, 2022, **446**, 137004.
90 J. Lou, L. Xu, W. Ju, D. Wang, T. Cheng, W. Zhu, N. Su and J. Ding, *J. Mater. Chem. C*, 2024, **12**, 10660–10668.

View Article Online
DOI: 10.1039/D6SC03065C

91 Z. Chen, M. Li, Q. Gu, X. Peng, W. Qiu, W. Xie, D. Liu, Y. Jiao, K. Liu, J. Zhou and S. J. Su, *Adv. Sci.*, 2023, **10**, 2207003.
92 Z. Chen, Q. Gu, M. Li, W. Qiu, Y. Jiao, X. Peng, W. Xie, D. Liu, K. Liu, Z. Yang and S.-J. Su, *Adv. Opt. Mater.*, 2024, **12**, 2302503.
93 M. Li, W. Xie, X. Cai, X. Peng, K. Liu, Q. Gu, J. Zhou, W. Qiu, Z. Chen, Y. Gan and S.-J. Su, *Angew. chem. Int. Ed.*, 2022, **61**, e202209343.
94 J. Huang, H. Nie, J. Zeng, Z. Zhuang, S. Gan, Y. Cai, J. Guo, S.-J. Su, Z. Zhao and B. Z. Tang, *Angew. chem. Int. Ed.*, 2017, **56**, 12971–12976.
95 H. Liu, J. Zeng, J. Guo, H. Nie, Z. Zhao and B. Z. Tang, *Angew. chem. Int. Ed.*, 2018, **57**, 9290–9294.
96 Y. Fu, H. Liu, D. Yang, D. Ma, Z. Zhao and B. Z. Tang, *Sci. Adv.*, 2021, **7**, eabj2504.
97 H. Liu, Y. Fu, J. Chen, B. Z. Tang and Z. Zhao, *Adv. Mater.*, 2023, **35**, 2212237.
98 Y. Fu, H. Liu, B. Z. Tang and Z. Zhao, *Adv. Funct. Mater.*, 2024, **34**, 2401434.
99 S. Song, R. Sun, J. Zeng, X. Peng, B. Z. Tang and Z. Zhao, *Adv. Opt. Mater.*, 2025, **13**, e02168.
100 X. Wu, X. Peng, L. Chen, B. Z. Tang and Z. Zhao, *ACS Mater. Lett.*, 2023, **5**, 664–672.
101 X. Peng, P. Zou, J. Zeng, X. Wu, D. Xie, Y. Fu, D. Yang, D. Ma, B. Z. Tang and Z. Zhao, *Angew. Chem. Int. Ed.*, 2024, **63**, e202405418.
102 M. Yu, X. Wu, H. Liu, Z. Yang, N. Qiu, D. Yang, D. Ma, B. Z. Tang and Z. Zhao, *Adv. Sci.*, 2023, **10**, 2206420.
103 F. Tenopala-Carmona, O. S. Lee, E. Crovini, A. M. Neferu, C. Murawski, Y. Olivier, E. Zysman-Colman and M. C. Gather, *Adv. Mater.*, 2021, **33**, 2100677.
104 Z. Yan, W. Dong, X. Ma, D. Jiang, S. Ge and P. Lu, *Angew. Chem. Int. Ed.*, 2026, **65**, e25851.
105 S. Wu, T. Wang and E. Zsyman-Colman, *CCS Chem.*, 2024, **6**, 2727–2740
106 S. Kong, H. Wang, J. Liao, Y. Xiao, T. Yu and W. Huang, *Adv. Mater.*, 2024, **36**, 2412468.

Data sharing not applicable – no new data generated.

View Article Online
DOI: 10.1039/D6SC03065C